COLLISION OF COMET SHOEMAKER--LEVY 9 WITH JUPITER: IMPACT STUDY OF TWO FRAGMENTS FROM TIMING OF PRECURSOR EVENTS

ZDENEK SEKANINA

Jet Propulsion Laboratory
California Institute of ~'ethnology
Pasadena, California 91109

Presentation at the IAU Colloquium No. 156
The Johns Hopkins University
Baltimore, Maryland
9--12 May 1995

To be submitted to Icarus

April 1995

Abstract

The impacts of fragments K and R of comet Shoemaker-Levy 9 are examined with the aims to interpret the timing of the observed precursors to the main thermal emission event and to correlate the results of ground-based infrared observations with a variety of observations made onboard the Galileo spacecraft. Analysis of the phenomena associated with the impact and explosion of fragment K shows that there is no discrepancy in the timing of the Earth- and Galileo-based observations and that the time of 53 ± 3 seconds between the emission peak of Precursor 1 and the onset of Precursor 2, as recorded by terrestrial observers, can be interpreted as the interval between the impactor's disappearance behind the Jovian limb and the first appearance of the ejects's plume over the limb following the explosion of the fragment's residual mass, It is concluded that the impactor exploded at an altitude of 45 to 50 km above the pressure level of 1 bar and that the residual mass involved in the explosion, approximately 6 to 7 million tons and about 400 meters across, represented only a fraction of 1 percent of the fragment's preatmospheric mass. The explosion is calculated to have taken place under a dynamic pressure of several hundred bars and the dissipated energy is found to have been on the order of 10^{26} erg. The results for fragment R show it to be smaller and less massive than fragment K, exploding slightly higher in the Jovian stratosphere, 50–60 km above 1 bar. The preferred solutions suggest that the rate of ablation of these impactors was comparable with, or somewhat higher than, that of category IIIb fireballs in the Earth's atmosphere. These fireballs represent a population of objects consisting of "soft" cometary material, whose bulk density is typically 0.2 g/cm^3. Preliminary evidence from other observations of the various fragments appears to be consistent with the present conclusions. All plume-expansion models based on penetrations below the clouds are incorrect and need major revisions. The successful prediction of explosion altitudes for the Shoemaker-Levy 9 fragments, based on the slightly modified fundamental actuations of the classical theory of meteor physics and on ablation rates derived from data on relevant terrestrial fireballs, is a tribute to the meteor theory and demonstrates the versatility of its techniques in applications.

1. INTRODUCTION

Independent observations of the impact phenomena associated with the collision of Jupiter with fragments K and R of comet Shoemaker--Levy 9 are combined in this study to investigate the characteristics of these events. In par titular, efforts are made to reconcile the timing of the first and the second precursors of the K impact (each showing up as a flash), derived from ground-based observations of high temporal resolution, with the timing of the luminous event observed from the Galileo spacecraft. The recently proposed interpretation of ground-based observations (Hamilton *et* al. 1995), which identifies the first precursor with the impactor's penetration (the meteor phenomenon) and the second precursor with the expanding cloud of ejects from the terminal explosion, is refined by recognizing specific signatures of the impactor and the rising plume of the ejects. It will be investigated whether this relationship allows one to constrain the penetration depth and the bulk properties of the impactor.

The impact events were characterized by the fact that all phenomena occurring below certain altitudes could not be directly observed from Earth because they took place on the far side of Jupiter. The critical altitudes were ~300- 400 km above the pressure level of 1 bar for K and much less for R (Chodas 1995), depending on the elevation of the uppermost level of the Jovian atmosphere that appreciably attenuates the light, of a given wavelength, from a source viewed from Earth over the planet's limb. In the most conservative case for the visual region of the spectrum, onc could identify this attenuation layer with the ammonia cloud tops, at a pressure of 400--500 mbar. In a more likely scenario, however, the existence of a haze above these clouds shifts the effective opacity boundary toward lower pressures, perhaps near 100 mbar (Chodas 1995).

2. IMPACTOR'S DISAPPEARANCE AND EXPLOSION AND EJECTA PLUME'S APPEARANCE

Close examination of the precursor timing requires sampling of high temporal resolution. Among observations of the K event, I found this constraint to be satisfied by a dataset obtained in a spectral region centered on 2.35 μm with the It-%-cm reflector of the Okayama Astrophysical Observatory on July 19, 1994 (Watanabe *et al.* 1995, Takeuchi *et al.* 1995). The monitoring consisted of a sequence of frames, each of one-second exposure time and taken at an approximate rate of six per minute. Tile reported results, giving the beginning times of exposure, indicate that the first detection of Precursor 1 occurred at 10:24:02 UT ancl that the signal peaked within 10 seconds of this time, followed by a gradual decrease to a minimum at 10:24:58 UT. Precursor 2 began with a steep rise of the signal, first detected at 10:25:08 UT and resulting in a well defined maximum around 10:25:26 UT. Another minimum followed at 10:26:15 UT and then the flux kept increasing at variable rates until about 10:38:37 U']', at which time the measured signal was ~3 orders of magnitude higher than the peak flux of Precursor 1. Parallel imaging-spectrometer observations by Meadows *et al.* (1995) indicate that the 2.3 μm flux was dominated by continuum emission, evidently of thermal origin, in the early phase of the K event's temporal evolution.

Consider a comet fragment striking the Jovian atmosphere with a speed of ~60 km/s. Three facts---all of them well known from meteor physics----are critical for understanding thermal emission variations in the event's precursor phase: (1) as the impactor penetrates supersonically into ever deeper and denser atmospheric layers, its temperature continues to increase due to friction with the shocked gas it encounters; (2) as a result of this interaction

with a column of the atmosphere, some of the object's kinetic energy is transferred to the atmosphere; and (3) because of the rapidly increasing dynamic pressure already at very high altitudes, the impactor's effective frontal area grows dramatically along its atmospheric path, as the object is subjected to progressively increasing fragmentation (Sec. 4). Fragmentation is one of the ablation processes and its effects are extensively documented in meteor phenomena, including those associated with very massive objects striking the Earth's atmosphere (e.g., Ceplecha *et al.* 1993).

The outlined sequence of events implies that once a fragment of the comet enters the Jovian atmosphere, the thermal emission observed from Earth begins to increase rapidly with time until, at a critical altitude Z_V, the object disappears behind the planet's limb. From this time on, the declining signal detected by Earth-based sensors is due entirely to the ablated material left behind and a column of the disturbed atmosphere in the wake of the penetrating impactor. Accordingly, *the peak of Precursor 1 identifies the time of the impactor's disappearance behind the limb*, t_V. The rest of the trajectory is hidden from view of Earth-based detectors, including the point of explosion.

The mass involved in the explosion is instantly shattered and vaporized and, as it cools *down,* much of it is recondensed and driven in an expanding mushroom-shaped plume back into the upper atmosphere along the impactor's path. When the plume's leading boundary has reached a critical altitude Z_Λ, at which the ejects's thermal emission is first detected from Earth, the observed signal begins to increase rapidly. Hence, the onset *of Precursor 2 identifies the earliest time of the plume's appearance over the planet's limb*, t_Λ. Because of Jupiter's spinning, the two critical altitudes differ from each other and since the impacts had occurred shortly before their sites rotated into view from Earth, it always was $Z_\Lambda < Z_V$. If this interpretation is correct, the time interval between the impactor's disappearance and the plume's first appearance is an important parameter that provides information on the depth of penetration and on other signatures of the explosion phenomena.

The highlights of the proposed scenario are depicted schematically in Fig. 1. The upper panel displays the geometry at the times t_V and t_Λ, including *the* critical altitudes Z_V and Z_Λ. The lower panel exhibits the precursors on the thermal emission curve and identifies the times t_V and t_Λ.

Returning now to the Okayama thermal flux curve for fragment 1G on July 21, 1994, the best estimate for the peak time of Precursor 1 is $t_V = 10{:}24{:}09 \pm 2$ UT, while the best estimate for the onset time of Precursor 2 is $t_\Lambda = 10{:}25{:}02 \pm 2$ UT, so that the interval of time during which the object was hidden from view by terrestrial observers is most likely to be 53 ± 3 seconds.

There appears to be a clear correlation between these constraints and the timing of the luminous event, observed for the 1G impact with the camera onboard the Galileo spacecraft through a methane-band filter centered at 0.89 μm (Chapman *et al.* 1995). The first detection was reported to have taken place at 10:24:13 $\pm$ 2 UT (Earth Receive Time), with a sharp peak following only 5 seconds later, at 10:24:18 $\pm$ 2 UT. Identifying this peak with the explosion, one finds that it took the impactor only 9 ± 3 seconds to penetrate from a critical altitude of Z_V to the explosion point and that the ejecta plume needed 44 ± 3 seconds to attain a critical altitude Z_Λ. I will now investigate whether the interpretation of these temporal relations is plausible and, if it is, what constraints do they set on the altitude of the impactor's explosion.

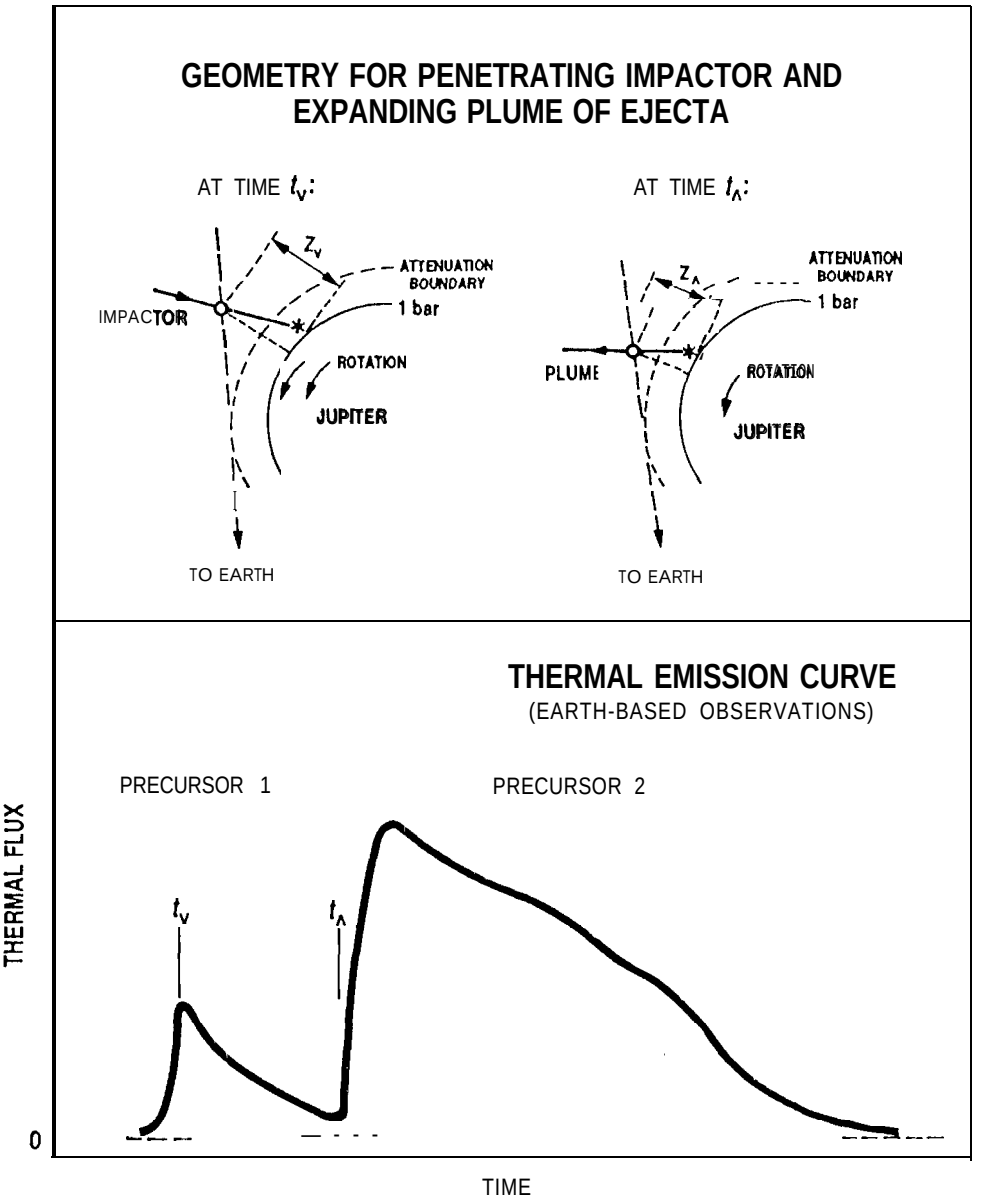

FIG. 1. Geometry considered for an impactor penetrating the Jovian atmosphere and for an expanding plume of the ejects (upper panel); and a schematic outline of the corresponding pre-main event portion of the thermal emission curve as observed from the ground (lower panel). As the impactor penetrates deeper into the atmosphere, its brightness increases until it disappears behind the limb when at an altitude Zv. The impactor's position is indicated by the open circle on the left-band side of the upper panel and the corresponding time t_V of the emission peak (Precursor 1) is derived from observations of high temporal resolution. Afterwards, the signal is due entirely to the wake of ablated material left behind and to a column of the disturbed atmosphere that trails the impactor and gradually cools down. The terminal explosion of tbe impactor's residual mass is hidden behind the limb and the observed signal continues to decline, until the front of the ejects's plume emerging from the point of explosion appears over the limb, at an altitude Z_Λ and time t_Λ. The plume's position at this time is shown by the open circle on the right-hand side of the upper panel. Because of Jupiter's spinning, the impactor's trajectory (along which the plume expands) rotates toward the terrestrial observer during the time interval between t_Λ and t_V, so that $Z_\Lambda < Z_V$. The thermal flux begins to increase dramatically at time t_Λ, the onset of precursor 2, when the expanding ejects's front first appears over the limb. The emission peak of Precursor 2 is determined by the balance between two competing effects, an increasing amount of plume material over the limb and its decreasing temperature; this time dots not, bowever, enter the considerations in this paper.

3, APPROXIMATIONS FOR IMPACTOR AND PLUME MOTIONS IN JOVIAN ATMOSPHERE

l'here is a consensus that any of the cornet's massive fragments could not be significantly dccele'rated by atmospheric friction before reaching the point of its explosion. Thus, if an impactor's velocity at the relevant altitudes is V and the zenith angle of its trajectory θ, the time the object needs to pierce the atmosphere from an altitude $Z_{\rm v}$, at time $t_{\rm v}$, to the altitude of explosion Z_*, at time t_*, is simply:

$$t_* - t_{\rm v} = -\frac{Z_* - Z_{\rm v}}{V \cos\theta} \tag{1}$$

The numerical simulations of hypervelocity impacts of kilometer-sized fragments of Shoemaker–Levy 9 and their explosions in the Jovian atmosphere (1 3oslough *et al.* 1994) have shown that in the early phase of plume expansion the debris front is strongly coupled with the shock front. Kompaneets (1 960), adapting the classical solution for a point source explosion to the case of an exponential atmosphere, also remarked that, as a *strong* shock propagates from the point of explosion, all the mass is concentrated in a thin shell at its front. The shock wave's upward expansion rate is

$$\left(\frac{dZ}{dt}\right)_{\rm shock} = \sqrt{\frac{\gamma+1}{2}\frac{p_{\rm shock}(Z)}{\rho_{\rm atm}(Z)}}, \qquad \lim_{t\to\infty}\left(\frac{dZ}{dt}\right)_{\rm shock} = \text{'-m'} \tag{2}$$

where γ is the specific heat ratio of the atmosphere, $p_{\rm shock}$ is the pressure behind the strong shock, and $\rho_{\rm atm}$ is the atmospheric density. The pressure $p_{\rm shock}$ is proportional to the total energy of the explosion and inversely proportional to the expanding cavity's volume (Zahnle & Mac Low 1994). When the explosion altitude is known, the differential equation (2) can be integrated numerically to determine the shock propagation. The calculations show that the shock velocity reaches a minimum soon after the explosion and then, as the, atmospheric density decreases, the strong shock accelerates beyond all limits. Bosloughet *al.*'s (1994) simulations have indicated that the debris gradually decouples from the shock front during the several tens of seconds after the explosion. The scenario in which plume material follows the shock wave with ever increasing delays is generally consistent with the llig}l-resolution observations made with the 1 Iubble Space Telescope (Hammel *et al.* 1995). These observations show the ejects reaching maximum elevations of ~3200 km, essentially independent of tile explosion energy. In ballistic terms, these peak altitudes imply an initial upward velocity of $U_\perp \simeq$ 13 km/s. Accordingly, I adopt a semi-empirical approach to approximating the ejects's motion: in the early phase of plume evolution, the material (essentially a superheated shocked gas) is assumed to expand with the shock front, with its motion corrected for effects of the ambient atmospheric pressure and Jupiter's gravity; after the decoupling, trajectories of the ejecta (cooled down substantially by then and largely recondensed into microscopic, particulate) are assumed to become ballistic, The transition of the plume's expansion from the shock regime to the ballistic regime is assumed to occur at an altitude $Z_{\rm b}$ and a time $t_{\rm b}$, for whit.]1 the two regimes yield the same critical upward plume velocity $U_{\rm crit}$, given by

$$\left(\frac{dZ}{dt}\right)_{\rm shock}\Bigg|_{t_{\rm b}} = U_\perp - g_{\rm J}\,(t_{\rm b} - t_*), \tag{3}$$

where $g_J \simeq 24.9\ \mathrm{m/s^2}$ is the! Jovian effective gravity at the relevant altitudes. The velocity variations are schematically outlined in Fig. 2. This approximation may overestimate the ejects's front velocity and therefore underestimate the time, but in terms of the duration of the shock regime, $t_b - t_*$, the effect cannot be very significant.

The duration of the ballistic regime, from the termination of the shock regime until the earliest time of plume appearance over the planet's limb, is equal to

$$t_\wedge - t_b = \frac{U_\perp}{g_J}\left(\sqrt{1 - \frac{2g_J Z_b}{U_\perp^2}} - \sqrt{1 - \frac{2g_J Z_\wedge}{U_\perp^2}}\right). \tag{4}$$

Finally, the entire period of time during which the impactor and the expanding plume could not be observed from Earth, $t_\wedge - t_\vee$, is given by the sum of the intervals $t_* - t_\vee$, $t_b - t_*$, and $t_\wedge - t_b$ from, respectively, Eqs. (1), (2) and (3), and (4) if $t_\wedge > t_b$, or by the sum of $t_* - t_\vee$ and $t_\wedge - t_*$ if $t_\wedge \leq t_b$.

4. Ablation, Altitude and Energy of Explosion, and Residual Mass

In his study of cosmic bombardment of Venus, Zahnle (1 992) defined an impactor's point of explosion in an exponential atmosphere by the condition of the maximum rate of energy dissipation per unit altitude interval. For the pressure p_* at the altitude Z_* he found

$$p_* = g_J \sqrt{\frac{2m\rho\cos^3 o}{3\pi H C_D}}, \tag{5}$$

where m, ρ, and C_D are the impactor's mass, bulk density, ant] drag coefficient, H is the pressure scale height, and O and g_J are the same quantities as in Eqs. (1) and (3), respectively. Although Zahnle & Mac Low (1994) applied this formula to calculate the explosion attitudes of the fragments of Shoemaker–Levy 9, there are two major problems with it when employed for poorly cemented objects. One, in deriving it, Zahnle (1992) neglected ablation, so that m in Eq. (5) is both the initial mass and the mass at the time of explosion. Two, while the postulated equivalence between the points of explosion and maximum energy dissipation is reasonable, observational evidence indicates that the velocity of a "soft" impactor at the point of its disintegration is grossly inconsistent with Zahnle's prediction for the point of maximum energy dissipation.

To address the two problems quantitatively, I refer to Borovička & Spurný's (1 995) study of the fireball Šumava (EN 041274), photographed from several stations of the *European Network* of fireball monitoring. At its maximum brightness, this category IIIb fireball reached panchromatic magnitude –21.5, normalized to a distance of 100 km. In the classification introduced by Ceplecha & McCrosky (1976), fireballs of category IIIb are recognized as having a low bulk density ρ (typically $\sim 0.2\ \mathrm{g/cm^3}$) ant] a high ablation coefficient $\sigma\ (\sim 0.2\ \mathrm{s^2/km^2})$. These fireballs represent the population of objects made of "soft" cometary material of highly variable strength (e.g., Ceplecha 1977a,b, 1987, 1988; ReVelle 1983) and are good morphological analogues for Shoemaker- Levy 9's fragments. Since Šumava is the most massive cometary fireball on record, for which much information is available, Borovička & Spurný's findings on this object's properties are relevant to studies of the nature of the Jovian impacts in general and to efforts aimed at constraining the explosion attitudes in particular.

Borovička & Spurný conclude that the initial mass of Šumava was ~5 tons and find that the object's luminous trail began at an altitude of 99 km above sea level, where the dynamic pressure reached ~2 mbar and the atmospheric pressure was merely 0.4 μbar. An equivalent altitude in the Jovian atmosphere is ~380 km above 1 bar. The fireball disintegrated *entirely* by tile time it reached an altitude of 59 km (an equivalent Jovian altitude of ~190 krn above 1 bar), at a dynamic pressure of ~1 bar and an atmospheric pressure of 0.25 mbar. Its brightest flare was observed at an altitude of 67 km, where the dynamic pressure reached ~0.4 bar and the atmospheric pressure was 0.08 mbar. The fragments of Shoemaker-Levy 9 were subjected to the same dynamic pressure at an altitude of ~200 km above 1 bar, where the atmospheric pressure was ~0.15 mbar.

The Šumava fireball experienced only a minor terminal explosion, while the brightest flare took place about 0.7 second before the observed termination of the luminous trail. It is interesting to note in this context that some of the fragments of Shoemaker-Levy 9 (such as B, F, T, or U) failed to generate observable plumes. This result apparently implies that no appreciable mass was left in these cases to be involved in a terminal explosion because of relatively small preatmospheric masses, or particularly high ablation rates, or both. It is possible that bulk fragmentation events are the immediate cause for the absence of a detectable terminal explosion.

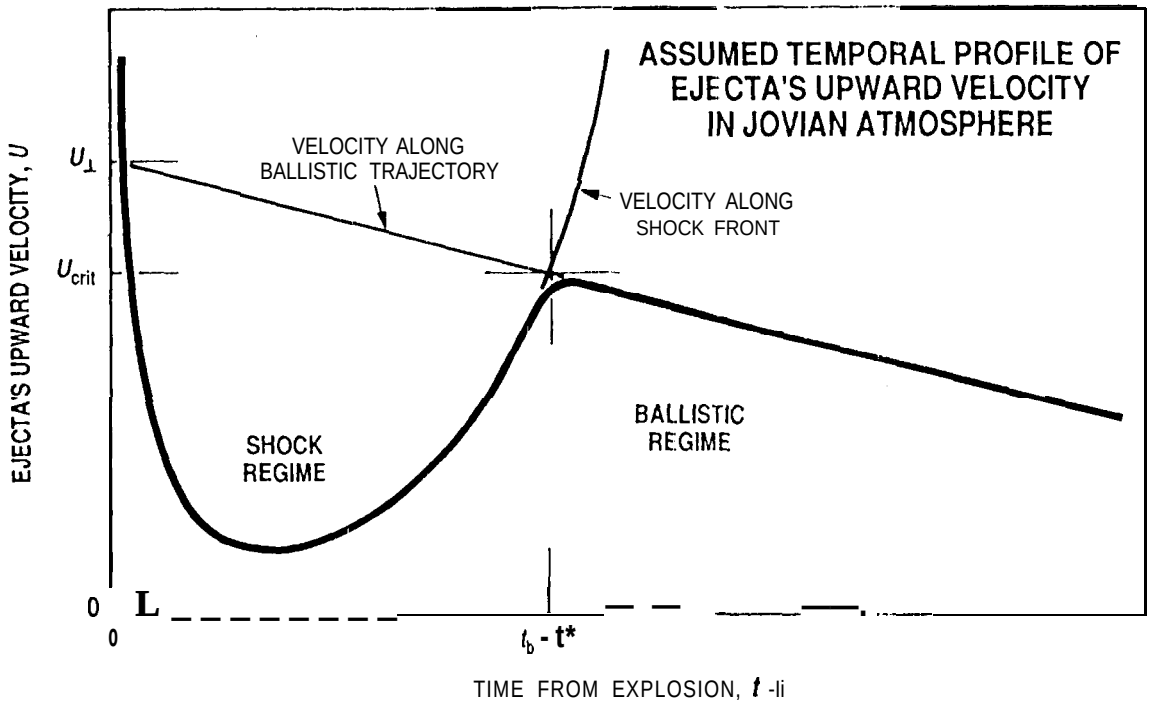

FIG. 2. Schematic outline of the assumed temporal profile of the upward velocity of tile ejects's front. In an early phase of plume development, the ejects are dynamically coupled with the shock wave and follow its expansion (shock regime).]n a late phase of development, the plume becomes decoupled from the shock wave, stays behind, and eventually follows a free-fall trajectory (ballistic regime), described by the Jovian effective gravity g_J aud an "initial" upward velocity $U_\perp$, related to the maximum altitude attained by the plume. It is assumed that the transition from the shock regime to the ballistic regime takes place at a time t_b, when the upward velocity reaches a critical value of U_{crit}. It is noted that an (obviously incorrect) assumption of the ejects following a ballistic. trajectory from the very explosion would severely overestimate both the expansion velocity and the penetration depth.

Continuous fragmentation is a major ablation mechanism for fragile impactors. It begins at low atmospheric pressures and is subsequently augmented-- often considerably-- by discrete events of *bulk fragmentation* that trigger major flares on the light curve. In terms of mass loss, fragmentation exceeds by orders of magnitude *thermal* ablation, which for massive objects not appreciably decelerated by atmospheric drag is insignificant. Thus, neglect of ablation, which was a "standard" assumption employed in numerous investigations of Shoemaker-I,evy 9 impacts, is unacceptable and cannot be defended.

The other problem with applying formula (5) to cometary impactors is the incorrect condition for the velocity at the time of explosion that is predicted by Zahnle's (1992) no-ablation model, namely, an $e^{-1/2}$ th part, or 0.61, the initial (preatmospheric) velocity. When one tests this prediction on Borovička & Spurný's (1995) results for the Šumava fireball, it fails miserably. Along the fireball's luminous trajectory the velocity was measured to decrease by 10 percent at the most, in good agreement with models that account for ablation, such as ReVelle's (1993) theory. Thus, the utter disagreement with Zahnle's model appears to be a direct consequence of the neglected ablation, not the assumed equivalence between explosion and maximum energy dissipation.

Zahnle & Mac Low's (1994) application of Zahnle's no-ablation model to the impacts of Shoemaker-I,evy's fragments into Jupiter further illustrates the kind of pitfalls that can only be avoided by abandoning the mode]. Using the values for the drag coefficient and the specific heat ratio preferred by Zahnle & Mac Low (C_D = 1.7 and γ = 1.2), I have been able to reproduce the explosion altitudes listed in their '1'able 1 to a few kilometers. However, I find that the tabulated values of the explosion energy are valid for a velocity of ~60 kill/s and are therefore inconsistent with the conditions On which the formula (5) was derived by Zahnle (]992); the energy should be lower by a factor of e = 2.718 . . . . The present results show (Sec. 5) that for some of the cases listed in Zahnle & Mac Low's Table 1 the plume's upward expansion is much too slow, by a factor of several, to explain the observed interval $t_\wedge - t_\vee$ of 53 seconds; while for the rest, the plume might not even have risen over the limb because of Jupiter's gravity, neglected by Zahnle & Mac Low.

I next compare the no-ablation model's results with those derived by Sekanina (1993), whose approach is semi-empirical. It is based on the fundamental equations of meteor physics, but the ablation coefficient employed is its mean *effective* value determined from reduced photographic observations of a large number of category IIIb fireballs. Although the *distribution* of fragmental ion events along the trail is unpredictable, all ablation is accounted for in this model. In addition, the classical theory is modified by allowing for progressively inceasing deformations in the shape of the impactor during its atmospheric flight (Chyba *et al,* 1993). *The* equations of motion, ablation, and deformation are then integrated side by side numerically, using very fine steps in time and other variables, such as velocity, frontal area, and residual mass. Values of the Jovian atmospheric pressure and density are taken from Orton's (1981) tables, which cover the attitudes from 1109 km above 1 bar down to 273 km below 1 bar. The impactor's tensile strength, to which the results are found to be insensitive, is assumed to be 0.01 bar, while the values used for the drag coefficient and tile specific heat ratio are those mentioned shove.

The ablation mode] employed by Sekanina predicts a cometary impactor's velocity at tile end of the luminous trail to be only marginally lower than its entry velocity, in substantial agreement with evidence from observations of category IIIb fireballs and with other paradigms that account for ablation, such as ReVelle's (1993) theory. The terminal

explosion for the impactor's given preatmospheric mass rn_o is predicted to occur much higher in the atmosphere than in Zahnle's scenario. The characteristic mass available at the time of explosion can be inferred from three different conditions, namely, as a residual mass (1) at the point of peak dynamic pressure, or (2) at the point of maximum energy dissipation per unit time, or (3) at the point of maximum energy dissipation per unit altitude interval. An encouraging feature is the fact that the three conditions yield nearly identical results, In relevant ranges of bulk density and explosion energy, the condition of peak dynamic pressure always results in the smallest value for the residual mass (as well as the lowest altitude), but the masses derived from the two energy dissipation conditions are greater, on the average, by a factor of only ~ 2. Differences among the three points in altitude and in time are entirely negligible, 0.1–0.3 km and less than 0.01 s, respectively. In the following, the point of peak dynamic pressure is employed to approximate the point of explosion. Using a nominal a, blation coefficient for category IIIb fireballs, $\sigma = 0.2\ s^2/km^2$, the calculated dynamic pressure at the point of explosion is found to be $\sim 1\,500$ bars for an impactor of a preatmospheric mass of $m_0 = 10^{16}$ g and a bulk density of $\rho = 0.2\ g/cm^3$. The peak dynamic pressure varies approximately as an 0.3 power of the explosion energy for a given density and as an 0.6 power of the density for a given explosion energy, with a tendency toward a lower power as the energy increases.

5. RESULTS AND D1scUSS1ON: FRAGMENT K

For a number of combinations of the impactor's initial mass m_0, effective diameter D_0, and bulk density ρ, Zahnle's no-ablation model has been compared with three ablation scenarios based on Sekanina's (1993) described approach. The coefficients of ablation selected for these scenarios are the nominal value of $0.2\,s^2/km^2$ for category IIIb fireballs and two "extremes" that differ from this value by a factor of two in either direction. The results are presented in Table 1 in terms of the impactor's residual mass rn*, diameter D_*, and its explosion energy E_* and altitude Z_*. The table's inspection indicates that differences in the characteristics m_*, D_*, E_*, and Z_* between the no-ablation case and any of the ablation scenarios are much greater than the differences among the various ablation scenarios. Specifically, in order to fit the same explosion altitude for a given bulk density, Zahnle's model requires the impactor's preatmospheric mass to be at least three orders of magnitude smaller than c1o the ablation scenarios. On the other hand, density effects on the characteristics m_*, D_*, E_*, and Z*, while by no means insignificant, are found to be somewhat smaller than the ablation effects.

The sensitivity of the results to tile ablation coefficient has majoi implications for sizes and masses of the fragments before they entered the Jovian atmosphere. However, for the given preatmospheric mass and bulk density, the explosion altitude varies only moderately with the ablation rate, *as long as it is comparable with the average rate for category IIIb fireballs*. The variations are always less than 30 km in the range of ablation scenarios considered in Table 1. By contrast, the disparity between the no-ablation case on the one hand and the ablation scenarios on the other hand is anywhere from ~ 55 km to ~ 150 km.

The average preatmospheric-to-residual mass ratio, m_0/m_*, *is* found to depend rather critically on the rate of ablation. The ratio varies from ~ 140 for an ablation coefficient of 0.1 s^2/km^2, to ~ 330 for 0.2 s^2/km^2, and to ~ 710 for 0.4 s^2/km^2. Correspondingly, the impactor's characteristic dimension at the time of atmospheric entry was ~ 5 to 9 times larger than its dimension at tile time of explosion. More than 99 percent of the object's

TABLE 1. Residual mass, effective diameter, energy, and altitude of Shoemaker-Levy 9 impactor at point of explosion as functions of initial conditions.

Impactor at time of atmospheric entry				Ablation dependent residue of impactor at time of terminal explosion (ablation coefficient σ in s^2/km^2)											
initial mass me(g)	kinetic energy E_0(erg)[a]	bulk density ρ (g/cm^3)	effective diameter Do(km)	residual mass m_* (g)				effective diameter D.(km)				explosion energy E_* (erg)				explosion altitude Z_*(km)[b]			
				σ=0[c]	σ=0.1	σ=0.2	σ=0.4	σ=0[c]	σ=0.1	σ=0.2	σ=0.4	σ=0[c]	σ=0.1	σ=0.2	σ=0.4	σ=0[c]	σ=0.1	C7=0.2	σ=0.4
10 *[3] 1	0[2 6" 2 4]	0.10	0.58	10^{13}	$10^{10.82}$	$10^{10.43}$	$10^{10.19}$	0.5S	0.11	0.080	0.067	$10^{25"81}$	1024"05	1023"6	$10^{23,43}$	22	79	91	105
		0.20	0.46		$10^{10.85}$	$10^{10.48}$	$10^{10.21}$	0.46	0.087	0.06$_6$	0.054		$10^{24.08}$	$10^{23.72}$	$10^{23.45}$	16	71	82	95
		0.30	0.40		$10^{10.86}$	$10^{10.50}$	$10^{10.12}$	0.40	0.077	0.059	0.044		$10^{24.10}$	$10^{23.74}$	$10^{23.37}$	12	66	77	89
		0.40	0.36		$10^{10.87}$	$10^{10.51}$	$10^{10.14}$	0.36	0.07$_1$	0.054	0.041		$10^{24.10}$	$10^{23.76}$	$10^{23.39}$	9	63	73	85
		0.50	0.34		$10^{10.88}$	$10^{10.52}$	$10^{10.16}$	0.34	0.06$_6$	0.050	0.038		$10^{24.11}$	$10^{23.76}$	$10^{23.41}$	6	60	70	82
1	0[14] 1	0.10	1.2	10^{14}	$10^{11.81}$	$10^{11.46}$	$10^{11.10}$	1.2	0.23	0.18	0.13	$10^{26.81}$	,	$10^{25.04}$	, $10^{24.70}$	$10^{24.34}$	-1	60	72	85
		0.20	1.0		$10^{11.80}$	$10^{11.48}$	$10^{11.13}$	**1.0**	0.18	0.14	0.11		$10^{25.03}$	$10^{24.72}$	$10^{24.38}$	–10	52	63	76
		0.30	0.86		$10^{11.81}$	$10^{11.49}$	$10^{11.15}$	0.86	0.16	0.13	0.10		$10^{25.05}$	$10^{24.73}$	$10^{24.39}$	–15	47	58	70
		0.40	0.78		$10^{11.82}$	$10^{11"50}$	1011"'6	0.78	0.15	0.11	0.088		$10^{25.06}$	$10^{24.74}$	$10^{24.40}$	–19	44	55	67
		0.50	0.73		$10^{11..93}$	$10^{11.48}$	$10^{11.16}$	0.73	0.14	0.10	0.082		$10^{25.06}$	$10^{24.72}$	$10^{24.41}$	–22	42	52	64
10^{15}	,.28.24	0.10	2.7	1	0[12"77]	1 0,2'46	10'2 3	2.7	0,48	0.38	0.30	$10^{27"81}$	1026'001	025"70	$10^{25"37}$	–33	44	55	68
		0.20	2.1		$10^{12.88}$	$10^{12.45}$	$10^{12.14}$	2.1	0,42	0.30	0.24		$10^{26.11}$	, $10^{25.69}$	, $10^{25.39}$	–45	36	47	59
		0.30	1.9		$10^{12.87}$	$10^{12.46}$	$10^{12.15}$	**1.9**	0.36	0.26	0.21		$10^{26.10}$	$10^{25.70}$	$10^{25.40}$	–52	31	42	54
		0.40	1.7		$10^{12.86}$	$10^{12.47}$	$10^{12.13}$	1.7	0.33	0.24	0.19		$10^{26.10}$	$10^{25.71}$	$10^{25.38}$	-58	27	39	51
		0.50	1.6		$10^{12"86}$	10:2'56	10:2 14	1.6	0.30	0.24	0.17		$10^{26.09}$	, $10^{25.61}$	, $10^{25.38}$	–63	25	36	48
10^{16}	~2924	0.10	5.8	10*	$10^{13.88}$	10	$10^{13.44}$	$10^{13.11}$	5.x	1.1	0.81	0.63	$10^{28.81}$	$10^{27.06}$	$10^{26.68}$	$10^{26.36}$	–78	28	41	53
		0.20	4.6		$10^{13.98}$	, $10^{13.53}$	, $10^{13.13}$	4.6	1.0	0.69	0.51		$10^{27.21}$	$10^{26.77}$	$10^{26.37}$	–93	20	32	45
		0.30	4.0		$10^{13"94}$	1 0	13.52	$10^{13.14}$	4,0	0.82	0.59	0.44		$10^{27.18}$	$10^{26.76}$	$10^{26.38}$	–105	14	27	40
		0.40	3.6		$10^{13.92}$	$10^{13.51}$	$10^{13.24}$	3.6	0.74	0,54	0.43		$10^{27.16}$	$10^{26.75}$	$10^{26.48}$	–114	10	24	36
		0.50	3.4		$10^{13.91}$	$10^{13.63}$	$10^{13.23}$	3.4	0.68	0.55	0.40		$10^{27.15}$	$10^{26.87}$	$10^{26.47}$	–120	6	21	34

[a] Calculated on assumption that impactor's velocity coincided with velocity of escape at altitude of 1000 km above 1 bar.
[b] Reckoned from atmospheric pressure level of 1 *bar*.
[c] Zahnle's model.

initial mass ablates (and virtually the same fraction of its initial energy dissipates) during atmospheric flight prior to the terminal explosion. The ablated mass is indiscriminately dispersed over vast volumes of the Jovian upper atmosphere.

Although none of the four explosion characteristics listed in Table 1 appears to be a sensitive tracer of the impactor's density in the ablation scenarios under consideration, the rate of plume expansion and therefore the time interval $t_\wedge - t_\vee$ determined from Earth-based observations is found below to be a useful discriminant of this kind when appropriately combined with the ablation rate.

The sets of solutions exemplified in Table 1 that satisfy the additional constraint of $t_\wedge - t_\vee$ = 53 seconds for fragment K were searched for by calculating first, for each selected ablation coefficient, the values of explosion altitude $Z_*(E_*, p; \sigma)$ over a two-dimensional "grid" of independent variables, the explosion energy and the impactor's bulk density. These grid values Z* were then fitted with polynomials of $\log E_*$, whose coefficients were determined as polynomials of log *p*. Next, the altitudes $Z_\vee$ and $Z_\wedge$, corresponding to the times of the impactor's disappearance and the plume's first appearance over the planet's limb (Sec. 2), were selected and $t_\wedge - t_\vee$ was calculated for each grid point $\{E_*, p, Z_*; CT\}$, following the approach outlined in Sec. 3. Finally, the grid points were interpolated to identify the solutions for which the calculated values of $t_\wedge - t_\vee$ were in the range of the observed values, between 50 and 56 s. Based on the currently best orbital elements for fragment K, the tables by Chodas (1995) yield $Z_\vee$ = 390 km and $Z_\wedge$ = 340 km in the case that the detectable dimming along a line of sight is caused by the stratospheric haze near a pressure level of 100 mbar. This attenuation limit is the same as that adopted by Hammel *et al.* (1995) in their investigation. It obviously is subject to some error, probably of a few tens of kilometers, due in part to the effects of refraction in the Jovian atmosphere. The implied uncertainty in $t_\wedge - t_\vee$ is then on the order of ± 1 s, within the observed value's uncertainty. During the integration of the plume's expansion, the magnitude of the pressure behind the shock front, p_{shock}, was closely monitored in terms of the atmospheric pressure, p_{atm} and the condition for a strong shock, $p_{shock} \gg p_{atm}$, was found to be satisfied in all investigated scenarios.

The results of this procedure for fragment K are plotted in Fig. 3 as bands of interpolated solutions that satisfy the condition $50\,s \leq t_\wedge - t_\vee \leq 56$ s for each value of the ablation coefficient. The solutions based on Zahnle's no-ablation model (σ = O) and satisfying the same condition are also plotted for comparison. The figure indicates that for a given explosion energy the no-ablation model requires a bulk density that is systematically lower, by a factor of 20 to 100, than the density implied by the ablation scenarios. Specifically, if fragment K were not subjected to ablation during its atmospheric flight, its density could not exceed 0.02 g/cm^3 for $E_* < 10^{27}$ erg in order to fit the observed range of the $t_\wedge - t_\vee$ values. The impactor's maximum density allowed by the Zahnle model is ~ 0.03 g/cm^3 for an explosion energy near 1028 erg. Such extremely low densities are of course meaningless.

By contrast, the three ablation scenarios predict for fragment K bulk densities in a general range from 0.05 to 1 g/cm^3 for explosion energies between 10^{26} and 1027 erg, thus including a set of plausible solutions. Additional constraints could be imposed by setting explicit limits on the ablation rate, the bulk density, and/or the explosion energy. For example, if ablation coefficients of 0.1 s^2/km^2 and 0.4 s^2/km^2 are both considered to be outside the realm of probable uncertainty, the bulk density of fragment K is restricted

by Fig. 3 to values from $\sim$0.1 g/cm^3 for an explosion energy of 10^{26} erg to $\sim$1 g/cm^3 for an energy of 1027 erg.

A more attractive avenue for further constraining the solutions in Fig. 3 is offered by an unpublished result for the preatmospheric size of fragment K, determined photometrically from an imaging observation with the Wide Field Planetary Camera 2 (WFPC-2) of the Hubble Space Telescope made on June 27, 1994, about three weeks before this fragment's collision with Jupiter. Analysis of a processed digital map of a central region of this condensation, kindly supplied by H. A. Weaver, Space Telescope Science Institute, has shown that for an assumed geometric albedo of 0.04 at a wavelength region defined by the used *R* filter, the detected signal implies the fragment's preatmospheric effective diameter of D_0 = 3.2 km. The approach employed is described in detail elsewhere (Sekanina 1995). The uncertainty of this result stems primarily from the object's unknown reflectivity

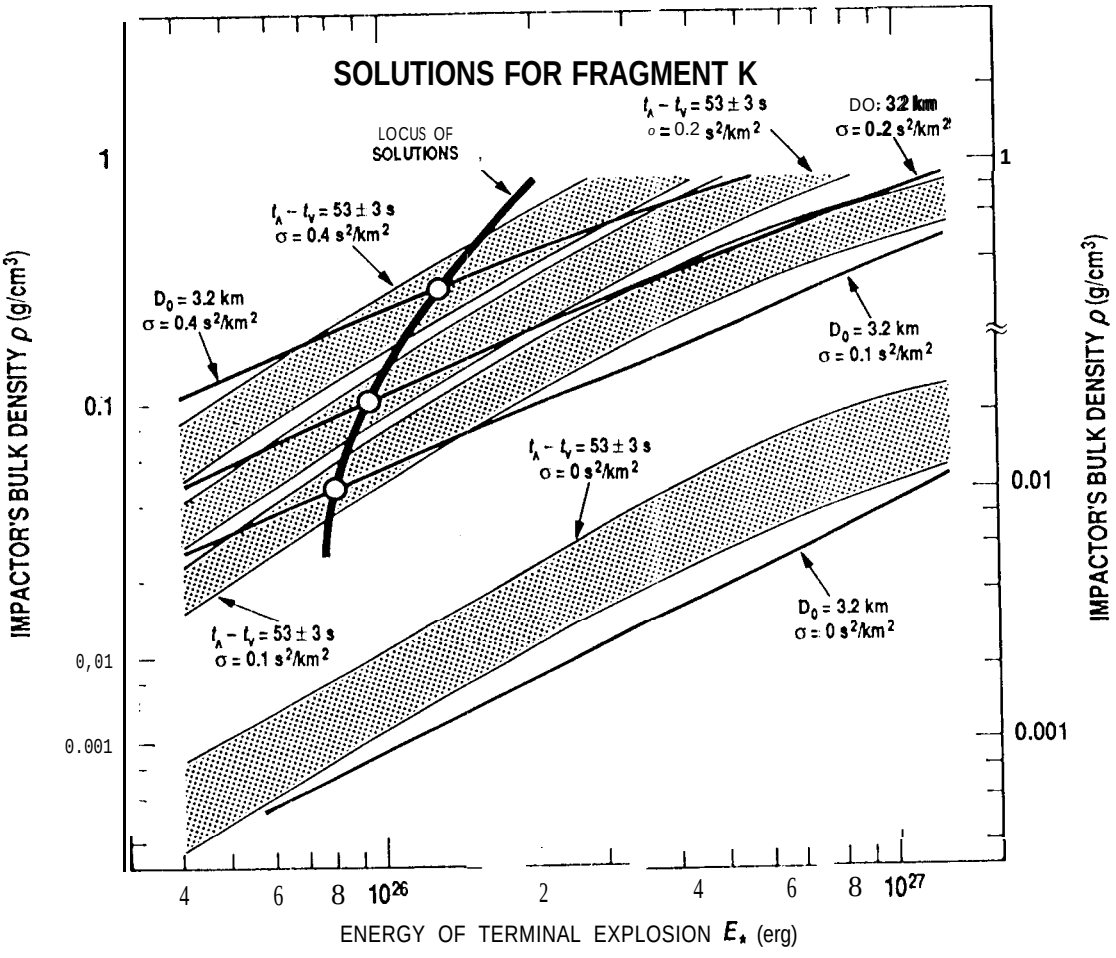

FIG. 3. Solutions to the explosion energy E_* and the bulk density ρ of fragment K for three ablation scenarios described, respectively, by the ablation coefficients σ of 0.1, 0.2, and 0.4 s^2/km and for a no-ablation case (Zahnle's model; σ = O). The shaded areas represent the solutions that satisfy a condition of 50 s < $t_A - t_V$ <56 s between the impactor's disappearance and the plume's first appearance, as recorded by Earth-based observers. The moderately heavy curves identify the solutions that are consistent with the fragment's preatmospheric effective diameter D_0 of 3.2 km, derived from images taken with the Hubble Space Telescope's WFPC-2. Finally, the very heavy curve depicts the solutions that satisfy both conditions, $t_A - t_V$ = 53 s and D_0 = 3.2 km.

and is estimated at approximately ±13 percent, if the error of the albedo is +0.01, The relationship between the explosion energy E_* and the impactor's bulk density p consistent with this effective diameter are represented in Fig. 3 by the curves that are identified by the D_0 value and the ablation coefficient. The most likely solutions, depicted by a heavy curve in the figure, are then defined by the points at which the D_0 curves intersect the central lines of the $t_\wedge - t_\vee$ solutions. The parameters at three points, corresponding to the selected ablation coefficients u, are listed in Table 2. The preferred solutions, with σ between 0.2 and 0.4 s^2/km^2, predict bulk densities of 0.2 ± 0.1 g/cm^3.

6. Results for Fragment R

When the present study of fragment K was near completion, a paper by Graham *et al.* (1995) was published on the R impact, describing 2.3 μm observations made with the W. M. Keck 10-meter telescope on July 21, 1994. The data, taken in a movie mode, with one frame of an integrated exposure of 4.3 s every 7.7 s, disclose the presence of two flashes preceding the main event, just as the Okayama observations do for fragment K. The first flash is characterized by a sharp peak at the time $t_\vee$ = 05:34:52.2 UT, while the second flash begins with a very steep rise of the signal at $t_\wedge$ = 05:35:46.4 UT. Hence, the time interval $t_\wedge - t_\vee$ = 54 seconds, with an estimated error of ±2 seconds, is virtually the same as that for fragment K. This coincidence is somewhat unexpected, since the R event was less prominent and occurred closer to the boundary between the planet's

Table 2. Nominal ablation scenarios for impacting fragment K of comet Shoemaker-Levy 9.

	Ablation coefficient u (s^2/km^2)		
	0.1	0,2	0.4
Impactor's Parameters at Time of Atmospheric Entry			
Preatmospheric mass, m_0 (g)	]014.91	$10^{15.27}$	$10^{15.69}$
Kinetic energy, E_0 (erg)"	10$^{28.15}$	$10^{28.51}$	$10^{28.93}$
Bulk density, ρ (g/cm^3)	0.047	0.11	0.29
Effective diameter, D_0 (km)	3.2	3.2	3.2
Impactor's Parameters at Time of Terminal Explosion			
Residual mass, m_* (g)	$10^{12.67}$	$10^{12.74}$	$10^{12.86}$
Residual energy, E_* (erg)	$10^{25.91}$	$10^{25.98}$	]026.10
Residual effective diameter, D_* (km)	0.57	0.46	0.36
Altitude above 1 bar, Z_* (km)	54	50	44
Ambient atmospheric pressure, p_* (bar)	0.066	0.080	0.11
Aerodynamic pressure, P (bar)	450	562	795
Preatmospheric-to-residual mass ratio, m_0/m_*	170	340	680
Preatmospheric-to- residual effective diameter ratio, D_0/D_*	5.6	7.0	8.8
Time Line of Events Occurring Hehind Jovian Limb			
Impactor's flight from disappearance to explosion, $t_* - t_\vee$ (s)	7.8	7.9	8.0
Plume's expansion in shock regime, $t_b - t_*$ (s)	38.5	38.0	37.2
Plume's expansion in ballistic regime, $t_\wedge - t_b$ (s)	6.7	7.1	7.8
Tots] time behind Jovian limb[b], $t_\wedge - t_\vee$ (s)	53.0	53.0	53.0

[a] Breed on assumption that impactor's velocity coincided with velocity of escape at altitude of 1000 km above 1 bar.
[b] Fitting the observed interval between $t_\vee$ = 10:24:09 UT and $t_\wedge$ = 10:25:02 UT on July 19, 1994, interpolated from available data (Watanabe *et al.* 1995, Takeuchi *et al.* 1995).

near and far sides, as viewed from Earth. However, it also should be remembered that a lower explosion energy entails a substantially lower upward shock-front velocity. It therefore appears that the competing effects nearly balanced each other in terms of the time involved, an interesting circumstance that is further examined below.

Graham *et al.*'s basic interpretation of the timing of the two observed flashes is similar to that employed in this study, except that they assume that the plume was on a ballistic trajectory with an initial upward velocity of ~8 km/s from the very time of explosion. Accordingly, they greatly overestimate the plume's early expansion velocity (Fig, 2) and necessarily also the impactor's penetration depth, which they readily admit. The present approach yields for the R event solutions listed in Table 3, based again on the precursor timing, They were constrained by the altitudes of the impactor's disappearance and the plume's appearance, Z_V = 245 km and Z_Λ = 210 km (Chodas 1995), and by the preatmospheric effective diameter of the fragment, for which an average value of D_0 = 2.4 km was obtained from analysis of WFPC-2 images taken in late January and late March 1994 (Sekanina 1995). Because of a lower explosion energy involved, the plume remained in the shock regime throughout its expansion phase behind the limb. This was a fortunate circumstance because the plume's ballistic parameter has not been well constrained for this event. The preferred solutions in Table 3 are again those for ablation coefficients between 0.2 and 0.4 s^2/km^2, predicting essentially the same range of bulk densities for the impactor as in the case of fragment K.

TABLE 3. Nominal ablation scenarios for impacting fragment R of comet Shoemaker–Levy 9.

	Ablation coefficient σ (s^2/km^2)		
	0.1	0.2	0.4
IMPACTOR'S PARAMETERS AT TIME OF ATMOSPHERIC ENTRY			
Preatmospheric mass, m_0 (g)	$10^{14.54}$	$10^{14.88}$	$10^{15.34}$
Kinetic energy, E_0 (erg)[a]	$10^{27.78}$	$10^{28.12}$	$10^{28.58}$
Bulk density, ρ (g/cm^3)	0.048	0.10	0.30
Effective diameter, D_0 (km)	2.4	2.4	2.4
IMPACTOR'S PARAMETERS AT TIME OF TERMINAL EXPLOSION			
Residual mass, m_* (g)	$10^{12.26}$	$10^{12.34}$	$10^{12.50}$
Residual energy, E_* (erg)	$10^{25.51}$	$10^{25.58}$	$10^{25.74}$
Residual effective diameter, D_* (km)	0.42	0.34	0.27
Altitude above 1 bar, Z_* (km)	Go	57	49
Ambient atmospheric pressure, p_* (bar)	0.049	0.058	0.085
Aerodynamic pressure, P (bar)	316	383	600
Preatmospheric-to-residual mass ratio, m_0/m_*	190	350	700
Preatmospheric-to-residual effective diameter ratio, D_0/D_*	5.7	7.0	8.9
TIME LINE OF EVENTS OCCURRING BEHIND JOVIAN LIMB			
Impactor's flight from disappearance to explosion, $t_* - t_V$ (s)	4.3	4.4	4.5
Plume's expansion from explosion to appearance[b], $t_\Lambda - t_*$ (s)	49.7	49.6	49.5
Total time behind Jovian limb[c], $t_\Lambda - t_V$ (s)	54.0	54.0	54.0

[a] Based on assumption that impactor's velocity coincided with velocity of escape at altitude of 1000 km above 1 bar.
[b] This expansion proceeded entirely in the shock regime; there was no ballistic regime.
[c] Fitting the observed interval between t_V = 05:34:52 UT and t_Λ = 05:35:46 UT on July 21, 1994 (Graham *et al.* 1995).

7. CONSTRAINTS FROM NEAR-INFRARED GROUND-BASED OBSERVATIONS

The models based on the precursor timing can further be tested on, and constrained by, available data on the near-infrared brightness of the impactors, interpreted as thermal emission. If a source's surface temperature is T, surface area S, emissivity ϵ, and distance to the observer A, its flux $\mathcal{F}_\lambda$, per unit wavelength interval, at a wavelength λ is

$$\mathcal{F}_\lambda = \frac{\epsilon S}{4\pi\Delta^2} c_1 \lambda^{-5} \left[\exp\left(\frac{c_2}{\lambda T}\right) - 1 \right]^{-1}, \tag{6}$$

where c_1 and c_2 are the blackbody radiation constants. In the following I express $\mathcal{F}_\lambda$ in units of erg/cm^3/s, λ in μm, S in km^2, T in deg K, and A in AU. The surface temperature is then related to the surface area by

$$T = \frac{14388.3}{\lambda \ln\left(1 + \frac{0.01336 S}{\mathcal{F}_\lambda \lambda^5 \Delta^2}\right)}. \tag{7}$$

The temperature is also constrained by an energy balance. The amount of energy that is transferred, per unit time, to an impactor of a frontal area A and velocity V is $\frac{1}{2}\Lambda\rho_{\rm atm} V^3 A$, where A is a dimensionless heat transfer coefficient and $\rho_{\rm atm}$ the local atmospheric density. The impactor's thermal radiation losses are given by $\epsilon\sigma_{\rm SB}(T^4 - T_{\rm atm}^4)S$, where $\sigma_{\rm SB}$ is the Stefan-Boltzmann constant. The fraction χ of the transferred energy that is spent on thermal reradiation is therefore approximately

$$\chi \simeq \frac{2\epsilon\sigma_{\rm SB}(T^4 - T_{\rm atm}^4)}{\Lambda\rho_{\rm atm} V^3}, \tag{8}$$

where it is assumed that the primary emitter of thermal radiation is the most involved surface, the frontal area ($S \simeq A$). Unfortunately, the determination of the heat transfer coefficient is rather uncertain. For fireballs entering the Earth's atmosphere, the problem of heat transfer was discussed extensively by ReVelle (1979), in cent inuum flow, which for kilometer-sized impactors in the Jovian atmosphere is valid at altitudes of up to at least 500 km above 1 bar, ReVelle found that convective heat transport dominates at higher altitudes for large impactors, while radiative transport prevails in deeper layers. For highly fragile objects—a case that is particularly relevant to comet Shoemaker–Levy 9—ReVelle suggested that there should exist major differences in the clominant heat transfer mechanism for larger ancl smaller fragments. If fragmentation occurs primarily in brief discrete events, as Borovička & Spurný's (1 995) results indicate for the Šumava fireball, sizes of individual fragments may decrease with time more rapidly than the mean free path. In extreme situations, this could locally result in brief reversal from continuum flow to free molecular flow for small fragments, with significant effects on heat transfer rates. ReVelle's tabulation of maximum values of the equilibrium radiative heat transfer coefficient shows an increase with increasing body size and his theory's application to the three photographed meteorite falls typically yielded A $\simeq$ 0.1, generally increasing to somewhat higher values at higher altitudes.

In practice, one can use Eqs. (7) and (8) to find the range of solutions that relate an effective temperature $T_{\rm eff}$ to an effective emitting surface area $S_{\rm eff}$ and satisfy an obvious

soft constraint of $\chi\Lambda << 1$. 'I'he tests are conducted on three observations. The peak flux of Precursor 1 on Graham *et al.*'s (1995) 2.3 μm light curve for fragment R provides the first data point. This flux, per unit frequency interval, is $\mathcal{F}_\nu = 0.43$ Jy, equivalent to $\mathcal{F}_\lambda = 2.4 \times 10^{-6}$ erg/cm^3/s. The relevant altitude is 245 km (Sec. 6), where $T_{atm} = 178$ K and $\rho_{atm} = 4.8 \times 10^{-9}$ g/cm3 The second observation is the point on Graham *et al.*'s light curve for fragment R that immediately precedes the flux peak of Precursor 1. This flux, which from the histogram in their Fig. 213 is found to be $\mathcal{F}_\nu = 0.24$ Jy or, equivalently, $\mathcal{F}_\lambda = 1.4 \times 10^{-6}$ erg/cm^3/s, is nominally a mean over the arc of the impactor's trajectory between 5.56 and 9.90 seconds prior to the time of peak emission. The corresponding altitudes are between 490 and 670 km above 1 bar. Because of the rapid increase in the signal with time, an '(effective" altitude is obviously much closer to the lower of the two boundaries and I adopt, somewhat arbitrarily, that this "mean" altitude is ~530 km, so that $T_{atm} = 318$ K and $\rho_{atm} = 8.3 \times 10^{-13}$ g/cm3 The third data point is the peak flux of the K event's Precursor 1, which is estimated at $\mathcal{F}_\lambda = 3.2 \times 10^{-6}$ erg/cm^3/s from Watanabe *et al.*'s (1995) 2.35 μm light curve in their Fig. 2 and which is assigned to the previously established altitude of 490 krn above I bar ($T_{atm} = 293$ K, $\rho_{atm} = 2.0 \times 10^{-12}$ g/cm^3). In each case the effective emitting surface S_{eff} is expressed in units of the preatmospheric frontal area A_0, equal to 3.2 km^2 for fragment R and 5.6 km^2 for fragment K.

The results of this exercise are summarized in Table 4, which shows that the condition of $\chi\Lambda << 1$ is satisfied at the altitudes near 500 km above 1 bar for both fragment R and I{ only if their effective temperature was lower than 1000 K and their effective emitting surface equal to at least several hundred km2 On the other hand, the same condition is satisfied by a large number of solutions for fragment R at the altitude of ~250 km above 1 bar and only soft constraints can be set on the emitting area from a condition that T_{eff} at ~250 km be higher than that at ~500 km. Although there may exist other explanations for this enormous emitting surface, I suggest that the tabulated results present further evidence for fragmentation at high altitudes, in concert with the proposed ablation model. Since the disintegration of a body into N identical fragments implies an increase by $N^{1/3}$ in the cross-sectional area, a ratio S_{eff}/A_0 of several hundred would suggest, in this simple-minded scenario, a breakup into millions to hundreds of millions of pieces if the entire

TABLE 4. Effective temperature T_{eff}, effective emitting area S_{eff} in units of preatmospheric frontal area A_0, and product $\chi\Lambda$ for Precursor 1 of fragments R and K.

Effective temperature T_{eff} (K)	Fragment R at altitude of 245 km		Fragment R at altitude of 530 km		Fragment K at altitude of 490 km	
	S_{eff}/A_0	$\chi\Lambda$	S_{eff}/A_0	$\chi\Lambda$	S_{eff}/A_0	$\chi\Lambda$
2610	1.0	0.0053	...	...	...	...
2000	2.1	0.0018	...	...	...	...
1750	3.4	0.0011	...	...	...	...
1500	6.3	0.00058	...	...	...	...
1250	15	0.00028	...	...	11	0.67
1000	51	0.00011	30	0.65	38	0.27
800	240	0.00005	140	0.26	180	0.11
700	750	0.00003	440	0.15	520	0.064

impactor disintegrated at once, Since only a fraction of its mass is ablated at a time, much larger numbers of much smaller fragments should be involved to fit the observed infrared flux. Although these numbers may seem excessive, they are consistent with the expected ablation rates if microscopic particles are the fragmentation's ultimate products.

8. Conclusions

It is concluded that the residual mass of fragment K, estimated at 6 or 7 million tons and representing about *0.2* percent of the object's preatmospheric mass, exploded at an altitude bet ween 45 and 50 km above the 1 bar pressure level, with an energy of $\sim$ 1026 erg and under a dynamic pressure of several hundred bars. With a bulk density of $\sim 0.2\,g/cm^3$, the residual object's effective diameter at the explosion time is estimated at $\sim$400 meters, but its shape was probably significantly flattened by the action of the aerodynamic forces. The atmospheric pressure at this point was about 100 mbar. The results are based on the assumption that the explosion occurred at the point of peak dynamic pressure; if it took place *earlier,* tile residual mass involved would be somewhat *greater* and the altitude a little *higher*. The results not only satisfy the precursor timing constraints (Watanabe *et cd.* 1995, Takeuchi *et al.* 1995), but they also match closely the time of peak brightness reported by Chapman *et al.* (19!)5) from observations made with the camera onboard the Galileo spacecraft. The scenarios proposed in Table 2 yield a nominal time of explosion of t_* = 10:24:17 UT, which agrees with the time of the sharp peak on the methane-band light curve to 1 second (Sec. 2). If the explosion slightly preceded tile peak (implying a brief brightening of the emerging ejects's plume imn iediatel y following the explosion), the time coincidence would be perfect. In any case, the adopted identification of the peak of Precursor 1 with the impactor's disappearance behind the Jovian limb and the onset of Precursor 2 with the appearance of the expanding ejects's plume over the limb is quantitatively consistent with the observed phenomena that were associated with the explosion of the residual mass, with no disagreement in timing between the ground-based and spat.ccraft observations.

Fragment K was ranked slightly lower than G by Weaver *et* al. (1995), based on the brightness of the condensations in May 1995. Comparison of the calculated effective diameters of the two fragments in late June and early July (Sec. 5 and Sekanina 1995) led to the same conclusion. Thus, the explosion of the residual mass of fragment G is likely to have occurred at a somewhat lower altitude than the explosion of fragment K. Carlson *et al.*'s *(1995b)* interpretation of the expanding plume associated with fragment G places the nominal point of explosion just below the tropopause, at an altitude of some 30-35 km above 1 bar, again in general agreement with the present results.

The residual mass of the smaller fragment R is found to have exploded a little higher in the Jovian stratosphere than K, most probably between *50* and 60 km above 1 bar, with an energy of 4 to 5 x 1025 erg. The object's effective diameter at the time of explosion is estimated at $\sim$300 meters and its mass at 2 to 3 x 10^{12} g. The time of explosion is found to be t_* = 05:34:57 UT on July 21, which differs by 11 seconds from the reference time, 05:35:08 UT, derived for this event by Carlson *et al.* (1 995a) from their observations made with the Near Infrared Mapping Spectrometer onboard the Galileo spacecraft. This difference is entirely tolerable, as Carlson *et al.* admit that their timing reference is rather uncertain, duc in part to a low signal-to-noise ratio, in part to an imperfect temporal distribution of their data, sampled at only seven points in a period of 100 seconds centered on the reference time.

Other avenues to constrain penetration depths of the fragments include observations at wavelengths sensitive to temperatures at critical altitudes and spectroscopy of diagnostic species. To avoid an overinterpretation of such data, it should be pointed out that a strong shock dots not expand only upwards, but, to a limited extent, also into deeper layers, Kompaneets (1960) showed that the maximum downward penetration in an exponential atmosphere is about 1.4 scale heights, which for Jovian altitudes between O and 100 km corresponds to ~30 km. Hence, if an impactor explodes at an altitude of, say, 40 km, its effects could still be "registered" by the atmosphere at an altitude as low as ~1 O km, that is, in the ammonia clouds. In addition, vertical convection triggered by a hypervelocity impact and explosion, an issue that is entirely outside the scope of this investigation, is likely to mix and redistribute the various species over some range of depths and thus further to complicate the chemical signature of the explosion.

Orton *et al.* (1995) reported impact site observations that were sounding a range of pressure levels in the Jovian atmosphere during and following the collisions. They found that at the impact site L, temperature perturbations at 150 mbar (nominal altitude of ~40 km) were significantly greater ant] persisting for much longer periods of time than those at 400 mbar (altitude of ~20 km). Hence, one may estimate that fragment L (whose impact site's prominence was, according to Hammel *et al.* 1995, in the same class as that of fragment K) probably clid not explode below an altitude of 40 to 50 km, which virtually coincides with the explosion altitude found from entirely independent considerations for fragment K in this study. Negative preliminary results have been reported by Gurwell *et al. (1994)* from their monitoring of a number of impact sites at continuum wavelengths of 3.0 mm and 3.38 mm, which probe pressure levels centered on 800 mbar (altitude of ~8 km); by Kundu *et al.* (1 994) from their millimeter wave observations sensitive to pressure levels from 0.5 to 2.5 bars (altitudes from 16 km down to –30 km); and by Grossman *et al. (1994)* from interferometric observations at wavelengths of 3 and 6 cm, which probe depths at pressure levels from 1 to 5 bars (altitudes down to –60 km).

The only strong (but not absolutely convincing) evidence for a deep penetration had first appeared to be implied by Nell *et al.*'s (1995) reported finding that the inferred large amounts of S_2 near the impact site G, detected spectroscopically with the Hubble Space Telescope's Faint Object Spectrograph a few hours after impact, could not be of cometary origin. The implications were that the mass derived from Jovian sulphur-bearing molecules, that the fragment presumably disturbed the NH_4SH clouds predicted at atmospheric pressure levels exceeding 1.2 bars (altitudes from --5 km to about –20 km), and that the explosion should have occurred below the ammonia clouds. However, in a note added in the proofs, Nell *et al.* concede that the S_2 abundances derived in their paper are overestimated by a factor of at least 10^2, in which case all observed sulphur could be of cometary origin ancl the argument for deep penetration is no longer compelling.

To summarize, I am at present aware of no evidence that would indicate that any of the fragments exploded at an altitude below 30 km or caused a detectable temperature disturbance in atmospheric layers at pressures of $\gtrsim$1 bar. Specifically, the present results for fragments K and R suggest an explosion altitude Z* of slightly less than 50 km above 1 bar for an explosion energy of 1026 erg and a rate of decrease of ~16 km in Z* per one orcler-of-magnitude increase in the explosion energy. It appears that for no impactor did the explosion energy exceed 1027 erg and that in each case it represented only a fraction of one percent of the kinetic energy at atmospheric entry. This huge effect is accounted for by

progressive dissipation of energy due to prolific mass ablation during atmospheric flight, dominated by fragmentation events. Severe impactor fragmentation likewise seems to be supported by evidence from Earth-based near-infrared light curves of the first precursors and it also may be responsible for the peculiar radial rays clearly apparent in the arc-shaped distribution of debris on the Hubble Space Telescope's images of the G impact site.

Although ignored by most investigators of the Jovian events, the problem of ablation by fragmentation was in the past repeatedly addressed by meteor physicists. A particularly thorough study was published by McCrosky & Ceplecha (1970), who demonstrated that spraying, spallation, and pressure fragmentation represent ablation mechanisms that take place in different thermal regimes. They also called attention to the importance of the process of bulk (gross) fragmentation, discussed more recently in considerable detail by Ceplecha *et al.* (1 993). Although McCrosky & Ceplecha's (1 970) interest, was primarily in applications to objects whose mass range was relevant to photographic fireballs and meteors, many of their conclusions—including those on the low-temperature processes involved—have broad ramifications and are, at least in general terms, highly pertinent to impact studies of comet Shoemaker-Levy 9 and essential to the understanding of the disintegration of its fragments relatively high in the Jovian atmosphere. And since the altitude of explosion represents a fundamental initial condition for any investigation of the expanding plume of ejects, one concludes that all models based on the assumption of an impactor's penetration below the cloud layers are bound to yield manifestly incorrect results and must be rejected.

The successful prediction of the Shoemaker- Levy 9 explosion altitudes in the Jovian atmosphere, based on slightly modified equations applied is studies of fireballs in the Earth's atmosphere and on ablation rates derived in these studies, is a tribute to the classical theory of meteor physics. The great versatility of its techniques is demonstrated by their validation both in a new environment and in a preatmospheric mass range that exceeds by about nine orders of magnitude the upper bound to the mass spectrum of "soft" impactors considered in past applications. The experience with the Jovian events shows that they obviously involved fragments of a cometary (as opposed to an asteroidal) object and underlies both the importance of atmospheric ablation processes and the need to distinguish among the greatly different morphological categories of impactors.

ACKNOWLEDGEMENTS

I thank J. Borovička for communicating his results on the Šumava fireball before their publication, P. W. Chodas for information on the line-of-sight altitudes, and H. A. Weaver for providing digitally processed images of the comet's condensations, secured with the WFPC-2 of the Hubble Space Telescope. This work is based in part on observations made with the NASA/ESA Hubble Space Telescope obtained at the Space Telescope Science Institute (STScI), which is operated by the Association of Universities for Research in Astronomy, inc., under contract, with the National Aeronautics and Space Administration. This research was carried out by the Jet Propulsion Laboratory, California Institute of Technology, under contract, with the National Aeronautics and Space Administration.

REFERENCES

Borovička, J. & Spurný, P. (]995). Radiation study of two very bright terrestrial bolides. These proceedings.

Boslough, M. B., Crawford, D. A., Robinson, A. C. & Trucano, T. G. (1 994). Mass and penetration depth of Shoemaker–Levy 9 fragments from time-resolved photometry. *Geophys. Res. Lett.* **21**, 1555--1.558.

Carlson, R. W., Weissman, P. R., Hui, J., Segura, M., Smythe, W. D., Baines, K. H., Johnson, T. V., Drossart, P., Encrenaz, Th., Leader, F. & Mehlman, R. (1995a). Some timing and spectra] aspects of the G and R collision events as observed by the Galileo Near Infrared Mapping Spectrometer. In *ESO Conf. & Workshop Proc. No.* 52, R. M. West & H. Boehnhardt, eds. (European Southern Observatory, Garching bei München), pp. 69-73.

Carlson, R. W., Weissman, 1'. R., Segura, M., Hui, J., Smythe, W. D., Johnson, T., Baines, K. 11., Drossart, P., Encrenaz, Th., Leader, I?. E. & the NIMS Science Team (1995 b). Galileo infrared observations of the Shoemaker-Levy 9 G impact fireball: A preliminary report. *Geophys.* Res. *Lett.*, in press.

Ceplecha, Z. (] 977a). Meteoroid populations and orbits. in *Comets, Asteroids, Meteorites: Interrelations, Evolution, and Origins,* A. H. Delsemme (University of Toledo, Toledo, Ohio), pp. 143-150.

Ceplecha, Z. (] 977 b). Fireballs photographed in Central Europe. *Bull. Astron. Inst. Czech.* 28, 328-340.

Ceplecha, Z. (1987). Numbers and masses of different populations of sporadic meteoroids from photographic and television records. *Publ. Astron. Inst. Czech. Acad. Sci. No.* 67, pp. 211-215.

Ceplecha, Z. (1 988). Earth's influx of different populations of sporadic meteoroids from photographic and television data. *J-lull. Astron. Inst. Czech. 39, 221-236.*

Ceplecha, Z. & McCrosky, R. E. (1976). Fireball end heights: A diagnostic for the structure of meteoric material. *J. Geophys. Res.* 81, 6257--6275.

Ceplecha, z., Spurný, P., Borovička, J. & Keclíková, J. (1993). Atmospheric fragmentation of meteoroids. *Astron. Astrophys. 279, 615-626.*

Chapman, C. R., Merline, W. J., Klaasen, K., Johnson, T. V., Heffernan, C., Belton, M. J. S., Ingersoll, A. P. & the Galilee) Imaging Team (1995). Preliminary results of Galileo direct imaging of S-L 9 impacts. *Geophys. Res. Lett.,* in press.

Chodas, P. W, (1 995). Height (km) above 100 mbar level to enter line of sight to Sun and Earth vs. time after impact (s) for selected fragments. Personal document.

Chyba, C. F., Thomas, P. J. & Zahnle, 1{. J. (1993). The 1908 Tunguska explosion: Atmospheric disruption of a stony asteroid. *Nature* 361, 40–44.

Graham, J. R., de Pater, I., Jernigan, J. G., Liu, M. C. & Brown M. E. (1995). The fragment R collision: W. M. Keck telescope observations of SL9. *Science 267, 1320-1323.*

Grossman, A. W., White, S. hi., Muhleman, D, O. & Gurwell, M. A. (1994), Microwave imaging of Jupiter's troposphere during impact with comet P/Shoemaker-Levy 9. *Bull. Amer. Astron. Sot. 26,* 1587. (Abstract.)

Gurwell, M. A., Muhleman, 1). O., Phillips, J. A. & Grossman, A. W. (1994). Millimeter imaging of the comet P/Shoemaker-Levy 9 impacts on Jupiter. *Bull. A mer. A stron. Soc.* 26, 1583. (Abstract.)

Hamilton, 1). P., Herbst, T. M., Boehnhardt, H. & Ortiz-Moreno, J. L. (1995). Ground-based infrared observations of the S1,-9 impacts: A physical interpretation. *Geophys.* lies. *Lett.*, in press.

Hammel, H. 1]., Beebe, R. F., Ingersoll, A. P., Or-ton, G. S., Mills, J. R., Simon, A. A., Chodas, P., Clarke, J. 1'., De Jong, E., Dowling, T. 1., Harrington, J., Huber, I,. F., Karkoschka, E., Santori, C. M., Toigo, A., Yeomans, D. & West, R. A. (1995). HST imaging of atmospheric phenomena created by the impact of comet Shoemaker-Levy 9. *Science* 267, 1288-1296.

Kompaneets, A. S. (1960). A point explosion in an inhomogeneous atmosphere. *Sov. Phys. Dokl.* 5, 46--48.

Kundu, A., Grossman, A. W. & de Pater, 1. (1994). Millimeter wave observations of the effects of Shoemaker- Levy 9 on the Jovian troposphere. *Bull. Amer. Astron. Sot.* **26**, 1588. (Abstract.)

McCrosky, R. E. & Ceplecha, Z. (1970). Fireballs and physical theory of meteors. *Bull. Astron. Inst. Czech.* 21, 271-2%.

Meadows, V., Crisp, D., Orton, G., Brooke, 'I'. & Spencer, J. (1995). AAT IRIS observations of the S1,-9 impacts and initial fireball evolution. In *ESO Conf. &* Workshop *Proc.* No. 52, R. M. West & H. Boehnhardt, eds. (European Southern Observatory, Garching bei München), pp. 1 2 9 - 1 3 4 .

Nell, 1{. S., McGrath, M, A., Trafton, L. M., Atreya, S. K., Caldwell, J. J., Weaver, H. A., Yelle, R. V., Barnet, C. & Edgington, S. (1 995). HST spectroscopic observations of Jupiter after the collision of comet Shoemaker–Levy 9. *Science* 267, 1307-1313.

Orton, G. S. (1 981). *Atmospheric structure in the equatorial region of Jupiter,* a report of the Galileo Working Group on Atmospheres, Subcommittee on Atmospheric Structure, pp. 9-13.

Orton, G., A'Hearn, M., Baines, K., Deming, D., Dowling, T., Goguen, J., Griffith, C., Hammel, H., Hoffmann, W., Hunten, D., Jewitt, D., Kostiuk, T., Miller, S., Nell, K., Zahnle, K., Achilleos, N., Dayal, A., Deutsch, L., Espenak, F., Esterle, P., Friedson, J., Fast, K., Barrington, J., Hera, J., Joseph, R., Kelly, D., Knacke, R., Lacy, J., Lisse, C., Rayner, J., Sprague, A., Shure, M., Wells, K., Yanamandra-Fisher, P., Zipoy, D., Bjoraker, G., Buhl, D., Golisch, W., Griep, D., Kaminski, C., Arden, C., Chaikin, A., Goldstein, J., Gilmore, D., Fazio, G., Kanamori, T., Lam, H., Livengood, T., MacLow, M .--M., Marley, M., Momary, T., Robertson, D., Romani, P., Spitale, J., Sykes, M., Tennyson, J., Wellnitz, D. & Ying, S.–W. (1995), Collision of comet Shoemaker–Levy 9 with Jupiter observed by the NASA Infrared Telescope Facility. Science 267, 1277--1282.

ReVelle, D. O. (1979). A quasi-simple ablation model for large meteorite entry: theory vs observations. *J. Atm. Terr. Phys.* **41**, 453–473.

ReVelle, D. O. (1 983). The role of porosity in modeling tile dynamics, ablation, and luminosity of fireballs. *Meteoritics* 18, 386.

ReVelle, 1). O. (1 993). The meteoroid/atmosphere interaction spectrum. In *Meteoroids and Their Parent Bodies*, J, Štohl & I. P. Williams, eds. (Astron. Inst. Slovak Acad. Sci., Bratislava), pp. 343-346.

Sekanina, Z. (1 993). Disintegration phenomena expected during collision of comet Shoemaker--I,evy 9 with Jupiter. Science 262, 382–387.

Sekanina, Z. (1 995). Nuclei of comet Shoen~aker-Levy 9 on images taken with the Hubble Space Telescope. In *ESO Conf.& Workshop Proc.* No. 52, R. M. West & 11. Boehnhardt, eds. (European Southern Observatory, Garching bei München), pp. 29--35.

Takeuchi, S., Hasegawa, 11., Watanabe, J., Yamashita, T., Abe, M., Hirota, Y., Nishihara, E., Okumura, S. & Mori, A. (1995). Near-11{ observation of the cometary impact into Jupiter: Time variation of radiation from impacts of fragments C, I), and K. *Geophys.* lies. *Let* i.., in press.

Watanabe, J., Yamashita, T., Hasegawa, H., Takeuchi, S., Abe, M., Hirota, Y., Nishihara, E., Okumura, S. & Mori, A. (1995). Near-IR observation of cometary impacts to Jupiter: Brightness variation of impact plume of fragment K. *Publ. Astron.* Sot. *Japan*, in press.

Weaver, H. A., A'Hearn, M. F., Arpigny, C., Boice, D. C., Feldman, P. D., Larson, S. M., Lamy, 1'., Levy, D. H., Marsden, B. G., Meech, K. J., Nell, K. S., Scotti, J. V., Sekanina, Z., Shoemaker, C. S., Shoemaker, E. M., Smith, T. E., Stern, S. A., Storrs, A. D., Trauger, J. T., Yeomans, D. K. & Zellner, B. (1995). The Hubble Space Telescope (HST) observing campaign on comet Shoemaker–Levy 9. Science 267, 1282-1288.

Zahnle, K. J. (1 992). Airburst origin of dark shadows on Venus. *J. Geophys. Res.* **97**, 10243-10255,

Zahnle, K. & Mac Low, M.-M. (1994). Tile collision of Jupiter and comet Shoemaker–Levy 9. *Icarus 108, 1--17.*